

# Functional implications of calcium permeability of the channel formed by pannexin 1

Fabien Vanden Abeele, Gabriel Bidaux, Dmitri Gordienko, Benjamin Beck, Yuri V. Panchin, Ancha V. Baranova, Dmitry V. Ivanov, Roman Skryma, and Natalia Prevarskaya

Institut National de la Santé et de la Recherche Médicale, U800, Equipe labellisée par la Ligue Contre le Cancer, Université des Sciences et Technologies de Lille, Villeneuve d'Ascq Cedex, F-59655 France

**A**lthough human pannexins (PanX) are homologous to gap junction molecules, their physiological function in vertebrates remains poorly understood. Our results demonstrate that overexpression of PanX1 results in the formation of Ca<sup>2+</sup>-permeable gap junction channels between adjacent cells, thus, allowing direct intercellular Ca<sup>2+</sup> diffusion and facilitating intercellular Ca<sup>2+</sup> wave propagation. More intriguingly, our results strongly suggest that PanX1 may also form Ca<sup>2+</sup>-permeable channels in the endoplasmic reticulum (ER). These channels contribute to the ER Ca<sup>2+</sup> leak and

thereby affect the ER Ca<sup>2+</sup> load. Because leakage remains the most enigmatic of those processes involved in intracellular calcium homeostasis, and the molecular nature of the leak channels is as yet unknown, the results of this work provide new insight into calcium signaling mechanisms. These results imply that for vertebrates, a new protein family, referred to as pannexins, may not simply duplicate the connexin function but may also provide additional pathways for intra- and intercellular calcium signaling and homeostasis.

## Introduction

Intercellular channels, which cluster together to form gap junctions, are involved in various physiological functions (e.g., adaptation of retinas to the dark, conduction of excitation in the heart, and suppression of cell proliferation in cancer tissues). For vertebrates, gap junctions are formed by connexins, a multigene family of which 20 members have been identified in humans (Willecke et al., 2002). A new family of gap junction molecules, which are unrelated to connexins, has been identified in insects and nematodes and named innexins (Phelan et al., 1998).

We have recently demonstrated the presence of innexin homologues in various taxonomic groups, including vertebrates (Panchin et al., 2000; Panchin, 2005). Given the ubiquitous distribution of this protein family in the animal kingdom, we termed these proteins “pannexins” (PROSITE accession number PS51013; [www.expasy.org/prosite](http://www.expasy.org/prosite)). Three genes, pannexin-1 (PanX1), -2 (PanX2), and -3 (PanX3), have been cloned from the human and mouse genome, and the pattern of their expression in various tissues has been studied (Panchin et al., 2000; Bruzzone et al., 2003; Baranova et al., 2004; Panchin, 2005). It has been found that the human PanX1, which encodes mRNAs, are ubiquitously, although differentially, expressed in normal tissues. Human PanX2 is a brain-specific gene (Bruzzone et al., 2003; Baranova et al., 2004). Recently, it was demonstrated that in paired oocytes rodent PanX1, alone and in combination with PanX2, induced the formation of intercellular channels (Bruzzone et al., 2003). When expressed in a single *Xenopus laevis* oocyte, PanX1 hemichannels were shown to be functional in plasma membrane (Bruzzone et al., 2003; Bao et al., 2004). Pannexin membrane channels are mechanosensitive conduits for ATP (Bao et al., 2004). This type of nonjunctional function has been previously reported for connexins (for review see Stout et al., 2004). However, it is not clear if pannexins simply duplicate connexin functions or play some special physiological role.

F. Vanden Abeele, G. Bidaux, and D. Gordienko contributed equally to this paper.

Correspondence to Natalia Prevarskaya: [natacha.prevarskaya@univ-lille1.fr](mailto:natacha.prevarskaya@univ-lille1.fr)

Y.V. Panchin's present addresses are Institute for Information Transmission Problems, Russian Academy of Sciences, Moscow 101447, Russia; and the A.N. Belozersky Institute of Physico-Chemical Biology, Moscow State University, Moscow 119899, Russia.

D.V. Ivanov's present address is Dept. of Ophthalmology, Bascom Palmer Eye Institute, University of Miami Miller School of Medicine, Miami, FL 33136.

D. Gordienko's present address is Dept. of Basic Medical Sciences, St. George's University of London, London SW17 0RE, England, UK.

A.V. Baranova's present addresses are Dept. of Molecular and Microbiology, Georges Mason University, Manassas, VA 20110; and the Russian Academy of Medical Science, 123098 Moscow, Russia.

Abbreviations used in this paper: BODIPY, boron dipyrromethene difluoride; HEK, human embryonic kidney; ODN, oligodeoxynucleotide; RyR, ryanodine receptor; SERCA, sarcoplasmic/ER Ca<sup>2+</sup>-ATPase; TG, thapsigargin.

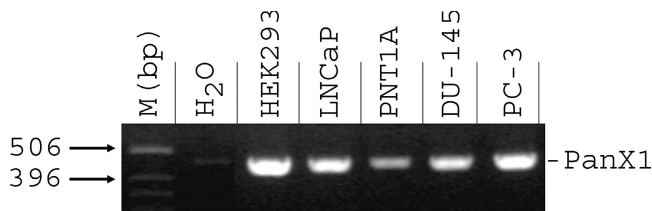


Figure 1. **Pannexin 1 (PanX1) mRNA is ubiquitously expressed in prostate cell lines.** 2% agarose gel showing the expression of the PanX transcripts in human prostate cell line: LNCaP, PNT1A, DU-145, and PC-3, as well as in HEK-293 cells. A no-template control (H<sub>2</sub>O) was also run with the PCR samples, where the cDNA was replaced with water.

In this work, we investigated the pannexin function in human cell lines transiently or stably transfected with pannexin (human PanX1). Our results demonstrate that overexpression of PanX1 enables the formation of Ca<sup>2+</sup>-permeable gap junction channels between adjacent cells, thus, allowing direct intercellular Ca<sup>2+</sup> diffusion and facilitating intercellular Ca<sup>2+</sup> wave propagation. Furthermore, we obtained evidence that strongly indicate that, in addition to the gap junction function, PanX1 overexpression increases the Ca<sup>2+</sup> permeability of the ER membrane and thereby affects intraluminal ER Ca<sup>2+</sup> concentration ([Ca<sup>2+</sup>]<sub>L</sub>). PanX1 overexpression dramatically reduces the intraluminal Ca<sup>2+</sup> content of the ER, which was directly measured by a fluorescent Ca<sup>2+</sup> indicator, Mag-fura-2. Endogenous PanX1 depletion by antisense and siRNA strategy in human prostate cancer cells increased the Ca<sup>2+</sup> content of the ER. Therefore, it seems likely that pannexins, which are structurally similar to gap junction-forming molecules, may also be involved in intracellular calcium homeostasis via the formation of the ER Ca<sup>2+</sup>-leak channels. These results give new insight into the mechanisms of the basal ER Ca<sup>2+</sup> leak, which has remained poorly understood until now.

Thus, the results of our study imply that where vertebrates are concerned, the pannexin family of gap junction proteins not only facilitates an intercellular Ca<sup>2+</sup> movement but also represents one of the mechanisms responsible for ER Ca<sup>2+</sup> leak.

## Results

In this study, we used human prostate cancer epithelial LNCaP cells (Vanden Abeele et al., 2002) and human embryonic kidney (HEK)-293 cells, which are classically used for heterologous transfection, as the experimental models.

### Pannexin cloning, endogenous expression in prostate cells lines, and localization

There are three distinct PanX genes: mammalian PanX1 mRNA is ubiquitously present in various tissues; PanX2 is a brain-specific gene; a low level of PanX3 has also been detected in the brain, and EST data suggest that PanX3 is expressed in osteoblasts and synovial fibroblasts (Panchin et al., 2000; Bruzzone et al., 2003; Baranova et al., 2004; Panchin, 2005). There is no indication of PanX2 or PanX3 expression in the prostate. The expression of PanX1 in the prostate has been shown by Northern blot of human tissues (Baranova et al., 2004). EST database inspection (<http://cgap.nci.nih.gov>) revealed five PanX1-related

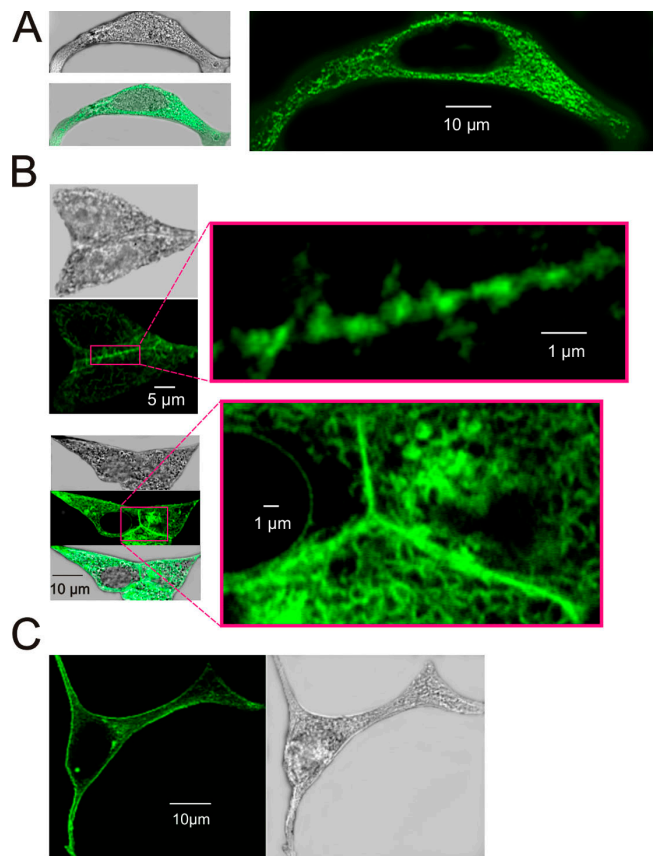
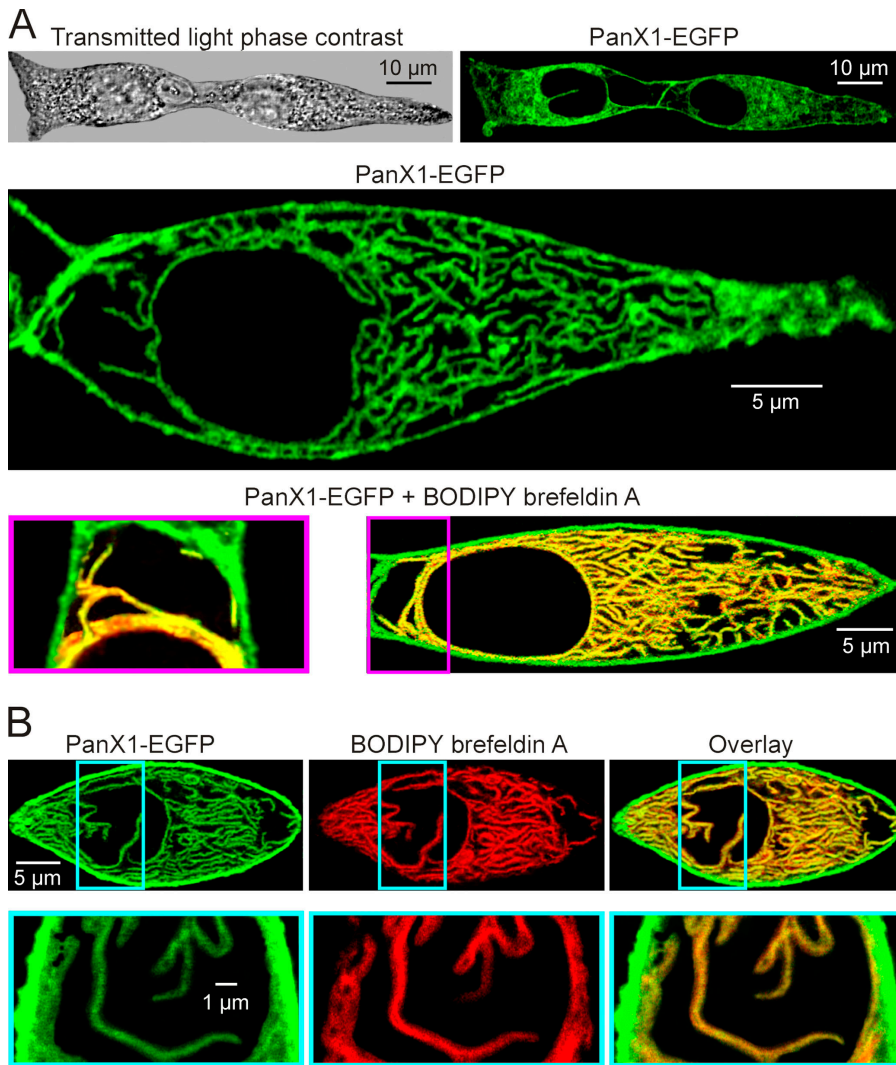


Figure 2. **Cellular localization of PanX1 in transiently transfected LNCaP cells.** (A) Fluorescent confocal images of LNCaP cells taken on the second day of transient transfection with pannexin1-pEGFP-N1 revealed that PanX1 protein is located in intracellular pools. (B) On the third day of transfection, PanX1-EGFP revealed distinct localization in the plasma membrane at the regions of cell-cell junction. Whole-cell views of the left part of the panel are a phase-contrast-transmitted light image, a GFP fluorescence confocal image, and their overlay. The boxed regions of interest taken at higher magnification are shown on the right. Note junctional plaques formed by the PanX1-EGFP. (C) 4 d after transfection, overexpression of PanX1-EGFP overloaded the plasmalemma, as can be judged by intense EGFP fluorescence outlining the cell membrane.

sequences from prostate cDNA libraries supporting this Northern blot data. Using RT-PCR, we have demonstrated the presence of PanX1 mRNA in LNCaP and HEK-293 cells used in our experiments (Fig. 1). The PanX1 fragment (encompassing what is believed to be the pore region of PanX1), was amplified by sequence-specific primers from 30 ng cDNA at 30 PCR cycles. Under control conditions, when RT was not added to the reaction, no product was amplified, even at 40 cycles. Because no antibodies to PanX1 are available, detection of the product expression at protein level is problematic.

To study the localization and the function of PanX1, we transiently overexpressed the PanX1-EGFP-fused protein in LNCaP and HEK-293 cells. PanX1 localization was verified using fluorescence confocal microscopy. 2 d after transfection, chimera were found to be exclusively intracellular and revealed a pattern consistent with that of the ER network (Fig. 2 A). 3 d after transfection, gathered cells displayed very thin and bright fluorescence at the regions of intercellular junctions furthest from intracellular staining. Fig. 2 B shows two groups of



**Figure 3. Cellular localization of PanX1 in stable cell line overexpressing PanX1-EGFP, (LNCaP-PanX1).** A representative pair of adjacent cells (transmitted phase-contrast image is shown on the top left in A) was chosen for confocal imaging. Spatial pattern of PanX1 distribution visualized with EGFP fluorescence (excited by the 488-nm line of argon laser; the fluorescence was captured at wavelengths 505–530 nm) was generally similar to that in transiently transfected LNCaP cells (see Fig. 2) and consisted of plasma membrane and intracellular pools with distinct expression of PanX1 in junctional regions (A, top left). A fluorescence confocal image of one cell from this pair taken at higher magnification and thinner confocal optical slice ( $<0.5 \mu\text{m}$ ) revealed that intracellular distribution of PanX1 is consistent with its localization in the ER; interconnected tubules forming a dense network are clearly seen in the confocal image of EGFP fluorescence (A, middle image). This was further confirmed by staining the cell with ER-specific marker BODIPY 558/568 brefeldin A (excited by the 543-nm line of HeNe laser; the fluorescence was captured at wavelengths  $>560 \text{ nm}$ ). The overlay of the EGFP and BODIPY brefeldin A fluorescence confocal images (A, bottom right) allows clear distinction between plasmalemmal (green) and ER (yellow) localization of PanX1. (A, bottom left) An enlarged boxed region (from A, bottom left) after rotation by  $90^\circ$ . Note that confocal images in top, middle, and bottom images were taken at different focusing (Z positions). Similar protocol was applied to another LNCaP cell. Confocal images of the EGFP and BODIPY brefeldin A fluorescence, as well as their overlay, are presented as indicated (B, top). The enlarged boxed regions taken at higher magnification are presented below each image after rotation by  $90^\circ$ , respectively (B, bottom). Note that the confocal images shown were obtained as a result of averaging of four sequential images taken in multitrack configuration of the confocal scanner followed by low-pass filtering ( $7 \times 7$  pixels; LSM 510 software) to improve the signal-to-noise ratio.

PanX1-EGFP-transfected LNCaP cells, and magnification of their tight cell-cell junctions revealed a dotted pattern similar to those of standard gap junctions. On day four, most of the cells overexpressed PanX1 in their entire plasma membrane, as shown in Fig. 2 C. Such intracellular and junctional localization of PanX1 is expected for a putative gap junction protein and suggests that our transient overexpression model reproduced the physiological pattern of endogenous pannexin distribution. Nevertheless, the abundance of PanX1 in the plasma membrane on the fourth day of the expression was probably caused by a protein overload of the membrane. Finally, to encounter the troubles caused by the low rate of transfection, we developed a stable cell line of LNCaP overexpressing PanX1-EGFP, referred to hereafter as “LNCaP-PanX1.”

Both transiently and stably transfected cells had similar PanX1 distribution patterns. This is further illustrated by Fig. 3, showing fluorescence confocal images of LNCaP-PanX1 in which the spatial arrangement of the ER network was visualized using specific ER marker boron dipyrromethene difluoride (BODIPY) 558/568 brefeldin A (Deng et al., 1995; Oh-hashii

et al., 2003). Interconnected tubules of the ER are clearly seen in EGFP and BODIPY brefeldin A fluorescence confocal images (Fig. 3). The overlay of the images allowed clear distinction between subplasmalemmal ER (which revealed both EGFP and BODIPY brefeldin A fluorescences) and plasmalemma (which shows EGFP fluorescence only), as illustrated in Fig. 3 (A and B, bottom). Thus, staining of LNCaP-PanX1 with BODIPY brefeldin A confirmed localization of PanX1 in the ER in these cells also.

#### Pannexin's intracellular leak-channel function

Because PanX1 is localized in the ER in both LNCaP and HEK-293 cells, we investigated whether PanX1 is involved in intracellular calcium homeostasis at ER level. To estimate the ER  $\text{Ca}^{2+}$  load and leak under PanX1 overexpression, we monitored changes in the cytosolic  $\text{Ca}^{2+}$  concentration ( $[\text{Ca}^{2+}]_i$ ) after the inhibition of sarcoplasmic/ER  $\text{Ca}^{2+}$ -ATPase (SERCA) with thapsigargin (TG). In these experiments, LNCaP and HEK-293 cells were loaded with the  $\text{Ca}^{2+}$  indicator fura-2. The application of

TG in  $\text{Ca}^{2+}$ -free external solution to control LNCaP cells unmasked a  $\text{Ca}^{2+}$  leak from the ER by inhibiting ER  $\text{Ca}^{2+}$  reuptake, which resulted in an increase in  $[\text{Ca}^{2+}]_i$  (Fig. 4 A). In PanX1-transfected cells, the amplitude of the TG-induced  $[\text{Ca}^{2+}]_i$  transient was dramatically smaller than that of control cells. This is summarized in the histograms in Fig. 4 B, where the amplitudes of TG-induced  $[\text{Ca}^{2+}]_i$  transients in control and under PanX1 overexpression in LNCaP and HEK-293 cells are compared. In both cell lines, the amplitude of the TG-induced  $[\text{Ca}^{2+}]_i$  transients was dramatically reduced in transfected cells; from  $690 \pm 68$  nM ( $n = 65$ ) to  $218 \pm 22$  nM ( $n = 43$ ) in LNCaP cells and from  $590 \pm 52$  nM ( $n = 61$ ) to  $200 \pm 40$  nM ( $n = 32$ ) in HEK-293 cells.

$[\text{Ca}^{2+}]_L$  was measured using the low-affinity  $\text{Ca}^{2+}$  indicator Mag-fura-2-AM, as previously described (Vanden Abeele et al., 2002). Imaging experiments with Mag-fura-2-AM were conducted on cells permeabilized by mild digitonin treatment. In PanX1-transfected LNCaP cells,  $[\text{Ca}^{2+}]_L$  was found to be reduced by 80% ( $70 \pm 30$   $\mu\text{M}$ ;  $n = 12$ ) in comparison to control cells ( $350 \pm 55$   $\mu\text{M}$ ;  $n = 15$ ; Fig. 4, C and D). At the end of the experiment, a high dose (1  $\mu\text{M}$ ) of a calcium ionophore ionomycin was added to assess the total calcium store content. Similarly, in HEK-293 cells, overexpression of PanX1 resulted in a reduction of  $[\text{Ca}^{2+}]_L$  by 73%;  $[\text{Ca}^{2+}]_L$  was  $300 \pm 40$   $\mu\text{M}$  ( $n = 36$ ) in control and  $80 \pm 29$   $\mu\text{M}$  ( $n = 16$ ) in transfected cells.

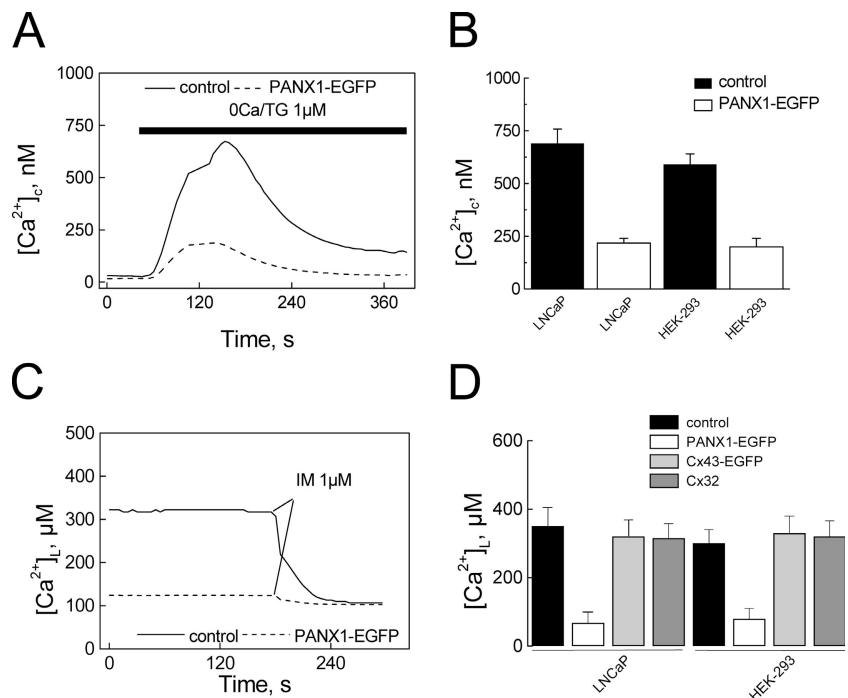
It has been previously demonstrated by Kumar et al. (1995) that overexpression of Cx32 ( $\beta 1$ ) in BHK cells may result in accumulation of assembled channels in the ER. To test whether the effect of pannexin overexpression on the ER  $\text{Ca}^{2+}$  leak could be mimicked by an overexpression of connexins, we analyzed the effect of connexin-32 protein (Cx32) and connexin-43 protein (Cx43) overexpression on the ER  $\text{Ca}^{2+}$  concentration ( $[\text{Ca}^{2+}]_L$ ) and compared these results with those

obtained with PanX1 overexpression. In these experiments, Cx32 and EGFP-fused Cx43 proteins were overexpressed in both LNCaP and HEK-293 cells, and  $[\text{Ca}^{2+}]_L$  was measured using the low-affinity  $\text{Ca}^{2+}$  indicator Mag-fura-2. In contrast to overexpression of PanX1, overexpression of Cx32 or Cx43 did not result in reduction of  $[\text{Ca}^{2+}]_L$  in either cell type (Fig. 4 D).

In another series of experiments, the ER  $\text{Ca}^{2+}$ -leak rate was assessed. Because  $[\text{Ca}^{2+}]_L$  was found to be, on average, 80% lower in cells transiently transfected with PanX1, the kinetics of the ER  $\text{Ca}^{2+}$  leak could not be evaluated by monitoring the time course of TG-induced decline in  $[\text{Ca}^{2+}]_L$  in these cells (Fig. 4, C and D). Therefore, we conducted this series of the experiments on LNCaP-PanX1 (cells stably transfected with PanX1), which showed only 20% reduction in  $[\text{Ca}^{2+}]_L$  in comparison with control cells (Fig. 5 A, top). To assess the kinetics of the ER  $\text{Ca}^{2+}$  leak, we monitored the time course of TG-induced decline in  $[\text{Ca}^{2+}]_L$  in digitonin-permeabilized LNCaP control cells (Fig. 5 A) and LNCaP-PanX1 cells with Mag-fura-2 (Fig. 5 C). From these measurements the rate of the ER  $\text{Ca}^{2+}$  leak (d. ratio/dt) was calculated (Fig. 5, B and D). LNCaP-PanX1 cells revealed a higher rate of  $\text{Ca}^{2+}$  leak than control cells, suggesting that PanX1 diminished ER  $\text{Ca}^{2+}$  content through an increase in passive  $\text{Ca}^{2+}$  leak from the ER. The validity of this approach has been justified in recent publications (Foyouzi-Youssefi et al., 2000; Pinton et al., 2000).

To evaluate a possible contribution of other  $\text{Ca}^{2+}$ -permeable ER channels, such as  $\text{InsP}_3$  receptors ( $\text{IP}_3\text{Rs}$ ) and ryanodine receptors (RyRs), to the ER  $\text{Ca}^{2+}$  leak in cells overexpressing pannexins, the rate of the ER  $\text{Ca}^{2+}$  leak in PanX1-transfected cells was measured in a solution supplemented with 100  $\mu\text{M}$  ryanodine (to inhibit RyRs) and 500  $\mu\text{g/ml}$  heparin (to inhibit  $\text{IP}_3\text{Rs}$ ) using a similar experimental approach. Inhibition of  $\text{IP}_3\text{Rs}$  and RyRs did not affect the rate of the ER  $\text{Ca}^{2+}$  leak (Fig. 5 E),

**Figure 4. PanX1 overexpression is associated with a reduction in the amount of  $\text{Ca}^{2+}$  that can be released from intracellular stores and the  $\text{Ca}^{2+}$  concentration within the ER.** (A) Two representative  $[\text{Ca}^{2+}]_i$  traces evoked by external application of 1  $\mu\text{M}$  TG in control (solid line) and PanX1-transfected (dashed line) LNCaP cells. (B) Amplitudes of TG-induced  $[\text{Ca}^{2+}]_i$  transients in control (filled bars) and under PanX1 overexpression in LNCaP and HEK-293 cells (open bars). Mean  $\pm$  the SEM. (C) Resting  $[\text{Ca}^{2+}]_L$  in control (solid line) and PanX1-transfected (dashed line) LNCaP cells. Please note that in both cases the calcium store was then depleted with 1  $\mu\text{M}$  ionomycin to assess the total calcium store content. (D) Resting  $[\text{Ca}^{2+}]_L$  (cumulative data; mean  $\pm$  the SEM.) for control (filled bars), PanX1/EGFP-transfected (open bars), Cx43/EGFP-transfected (light gray bars), and Cx32-transfected (gray bars) LNCaP and HEK-293 cells.



leaving PanX1 as the only molecule yet to be identified as being responsible for the ER Ca<sup>2+</sup> leak.

Furthermore, we performed a series of experiments to determine whether the overexpression of pannexins affects the level of Bcl-2, Bax, and Bak, which have been suggested as other potential Ca<sup>2+</sup>-leak channels (Camello et al., 2002; Oakes et al., 2005). The dot-blot experiments revealed that levels of Bcl-2, Bax, and Bak proteins were the same in the PanX1-transfected LNCaP cells as in control LNCaP cell (expressing EGFP only), thus, excluding a possible contribution of these molecules to the enhanced Ca<sup>2+</sup> leak also observed in LNCaP-PanX1 (Fig. 5 F). On the other hand, immunodetection experiments revealed that the EGFP detection level in LNCaP cells expressing PanX1-EGFP or EGFP only was a hundred times higher than that of the Bcl-2 family proteins. It is therefore unlikely that drastic change in Ca<sup>2+</sup> handling by the ER in LNCaP overexpressing PanX1 can be attributed to the expression of the Bcl-2 family proteins.

The question remains, however, as to whether endogenous PanX1 is actually involved in ER Ca<sup>2+</sup> leak. To test this, we compared the ER Ca<sup>2+</sup> content and kinetics of Ca<sup>2+</sup> leak from the ER in control LNCaP cells and in LNCaP cells subjected to a depletion of endogenous PanX1 protein using antisense and

siRNA technology (Khvorova et al., 2003). As shown in Fig. 6 A, siRNA-PanX1 reduced the endogenous PanX1 mRNA expression in HEK-293 cells. Western-blot revealed that siRNA-PanX1 also suppressed the PanX1 protein expression in LNCaP cells transfected with PanX1 (Fig. 6 B). Semiquantification revealed a decrease of  $42.38 \pm 7.06$  for 5 nM siRNA-PanX1 transfection (statistically different with control,  $P < 0.001$ ) and  $3.91 \pm 1.50$  for 100 nM (statistically different with both control and 5 nM siRNA,  $P < 0.001$ ), respectively. Given that siRNA treatment can cause effects unrelated to the depletion of the specific protein of interest, we tested the effect of the treatment with two different siRNA (directed against PanX1 and PanX1-unrelated murine TRPC6 protein) on ER Ca<sup>2+</sup> content in PanX1-transfected cells. As shown in Fig. 6 C, only siRNA-PanX1 partially restored ER Ca<sup>2+</sup> content in the LNCaP-PanX1 cell line, whereas siRNA had no effect against mTRPC6. The likely explanations for the fact that siRNA-PanX1 restored the ER Ca<sup>2+</sup> content only partially are that the siRNA transfection rate was  $\sim 80\%$  and the silencing efficiency of the siRNA was  $\sim 90\%$ .

The inhibition of PanX1 expression with specific siRNA increased [Ca<sup>2+</sup>]<sub>L</sub>. In LNCaP cells, [Ca<sup>2+</sup>]<sub>L</sub> measured with Mag-fura-2 was found to be on average 40% higher in

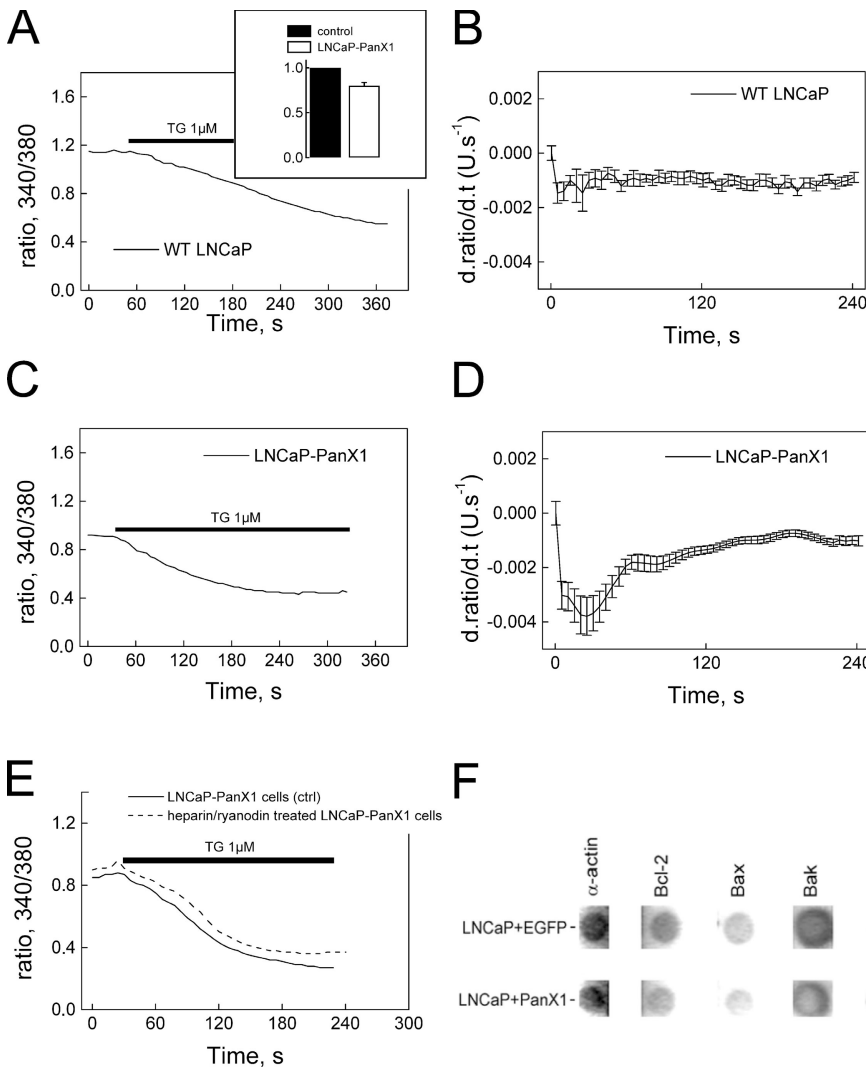
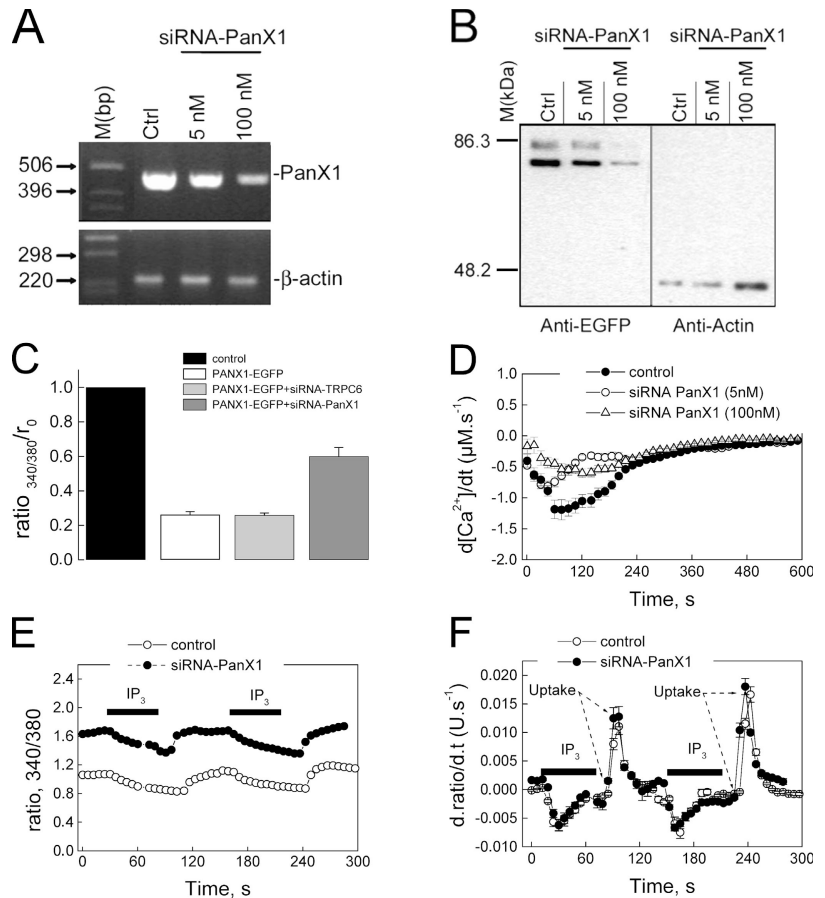


**Figure 5. Specific PanX1 overexpression induced an increase in passive Ca<sup>2+</sup> leak through the ER membrane.** (A and C) Addition of TG induced a slow reduction in [Ca<sup>2+</sup>]<sub>L</sub> in digitonin-permeabilized LNCaP and LNCaP-PanX1 cells. (B and D) Apparent Ca<sup>2+</sup>-leak rates are plotted as a function of time after TG application. The data in B and D are the mean  $\pm$  SEM for 15 and 17 cells, respectively. (E) ER Ca<sup>2+</sup> leak between PanX1-transfected cells and PanX1-transfected cells supplemented with 100  $\mu$ M ryanodine (to inhibit RyRs) and 500  $\mu$ g/ml heparin (to inhibit IP<sub>3</sub>Rs) revealed a similar rate. (F) Dot-blot experimentation ( $n = 2$ ) shows unchanged expression of the leak proteins Bcl-2, Bax, and Bak in EGFP-transfected LNCaP versus PanX1-transfected LNCaP. Actin was used as an internal standard for the amount of loaded proteins and GFP, similar to a reporter for EGFP and PanX1-EGFP transfection, respectively.

**Figure 6. PanX1 siRNA depletion increases the amount of Ca<sup>2+</sup> that can be released from intracellular stores and decreases the ER Ca<sup>2+</sup>-leak rate.** (A) siRNA-PanX1 reduced the endogenous PanX1 mRNA expression in HEK-293 cells. Semiquantitative RT-PCR (PanX1, 36 cycles;  $\beta$ -actin, 27 cycles) showing a decrease in the expression of the PanX1 transcripts in HEK-293 cells transfected for 2 d with 100 nM of siRNA-PanX1. Note that this reduction was not observed when the cells were incubated with vehicle only. The  $\beta$ -actin mRNA expression was used to control the RNA rate in each sample. (B) siRNA-PanX1 suppressed the overexpressed pannexin in LNCaP-PanX1 cells. Western-blot showing either a decrease or virtually complete suppression of the PanX1 protein in LNCaP-PanX1 cells transfected for 2.5 d with 5 and 100 nM of siRNA-PanX1, respectively. Note that the lower band corresponds to the expected 75-kD PanX1-EGFP, although the highest band could correspond to a posttranslational modification. Actin expression was used to control the amount of protein in each sample. (C) Effect of an unrelated siRNA treatment against murine TRPC6 protein on ER Ca<sup>2+</sup> content in PanX1-transfected cells. (D) Apparent rate of the ER Ca<sup>2+</sup> leak, plotted as a function of time after TG application in LNCaP cells treated with PanX1 siRNA for 48 h and in control cells. (E) The time course of [Ca<sup>2+</sup>]<sub>i</sub> changes (assessed with Mag-fura-2) induced by the transient extracellular application of IP<sub>3</sub> in digitonin-permeabilized cells. (F) Apparent rate of the ER Ca<sup>2+</sup> reuptake, plotted as a function of time after IP<sub>3</sub> washout in LNCaP cells treated with PanX1 siRNA for 48 h and in control cells.



PanX1-depleted LNCaP cells ( $495 \pm 30 \mu\text{M}$ ;  $n = 32$ ) than in control ( $340 \pm 50 \mu\text{M}$ ;  $n = 25$ ). To reveal the effect of depletion of endogenous PanX1 on the ER Ca<sup>2+</sup> leak, we calculated the rates of [Ca<sup>2+</sup>]<sub>i</sub> decline in response to TG application (measured with Mag-fura-2). PanX1-depleted LNCaP cells showed a significant decrease in the rate of ER Ca<sup>2+</sup> leak, suggesting a contribution of endogenous PanX1 to the ER Ca<sup>2+</sup> leak (Fig. 6 D).

In parallel experiments, we depleted endogenous PanX1 by the use of phosphorothioate anti-sense oligodeoxynucleotides (ODNs) and discovered a similar effect on ER Ca<sup>2+</sup> leak (not depicted).

Because ER Ca<sup>2+</sup> content is determined by the balance between Ca<sup>2+</sup> leak and reuptake, the possible effect of PanX1 overexpression on SERCA activity was tested (Fig. 6 E). The ER Ca<sup>2+</sup> uptake was investigated in digitonin-permeabilized cells using Mag-fura-2-AM, as previously described. The application of 100  $\mu\text{M}$  IP<sub>3</sub> triggered a rapid drop in [Ca<sup>2+</sup>]<sub>i</sub> caused by IP<sub>3</sub>-induced Ca<sup>2+</sup> release (Fig. 6 E). After IP<sub>3</sub> washout, the recovery of [Ca<sup>2+</sup>]<sub>i</sub> reflected reuptake of Ca<sup>2+</sup> into the ER (Fig. 6 E). The rate of the ER Ca<sup>2+</sup> reuptake (d. ratio/dt) was identical in control and PanX1 mRNA-depleted LNCaP cells (Fig. 6 F). Similarly, overexpression of PanX1 in either LNCaP or HEK-293 cells had no effect on Ca<sup>2+</sup> reuptake assessed in the same way (unpublished data). Therefore, we concluded that PanX1 overexpression has no direct inhibitory effect on SERCA.

Altogether, our results strongly suggest that PanX1 may form Ca<sup>2+</sup>-permeable channels in the ER membrane.

### PanX1 is a Ca<sup>2+</sup>-permeable gap junction channel

Our results demonstrate that: (a) PanX1 is expressed in the ER (Fig. 3) and plasma membranes (Figs. 2 and 3); (b) in plasma membrane, PanX1 is initially expressed in the junction areas between adjacent cells, where it may form gap junction plaques (as can be judged by nonuniformities of GFP fluorescence in these regions; Fig. 2 B); and (c) PanX1, when expressed in the ER membrane, forms Ca<sup>2+</sup>-permeable channels facilitating Ca<sup>2+</sup> leak from the ER (Figs. 4, 5, and 6). Therefore, we tested whether PanX1 may form Ca<sup>2+</sup>-permeable gap junction channels and thereby provide a pathway for direct intercellular Ca<sup>2+</sup> movement. To do so, we have monitored Ca<sup>2+</sup> movement from the dialyzed to the adjacent LNCaP cell by means of Ca<sup>2+</sup>-sensitive indicators and fluorescent confocal imaging. These experiments were conducted under conditions when the only source of Ca<sup>2+</sup> was a solution within the patch pipette, whereas all other mechanisms (except direct intercellular Ca<sup>2+</sup> movement), which can possibly contribute to generation of intercellular Ca<sup>2+</sup> waves, were pharmacologically suppressed (see following paragraph). One of the two adjacent cells was dialyzed through the patch pipette with a solution containing either 1  $\mu\text{M}$  Ca<sup>2+</sup> (Fig. 7, A and B) or 100  $\mu\text{M}$  Ca<sup>2+</sup> (Fig. 7, C-F), whereas changes in the fluorescence of the Ca<sup>2+</sup>-sensitive indicator (fluo-4 or rhod-2, respectively) were monitored in the dialyzed and adjacent cells using x-y confocal imaging. This experimental protocol was applied to LNCaP cells derived from

the line stably transfected with PanX1-EGFP (LNCaP-PanX1) (Fig. 7, A and C), from the line stably transfected with EGFP only ("LNCaP-EGFP"; Fig. 7 D), and from the control line (Fig. 7, B and E). In contrast to uniform EGFP fluorescence, which was observed when EGFP was solely expressed (Fig. 7 D), the fluorescence signal from EGFP coupled to PanX1 had distinct nonuniform cellular distribution, reflecting the expression of PanX1 in the ER and in the plasmalemma (Figs. 2, 3, 7 A, and C). The gap junction plaques formed by PanX1 clusters were clearly seen in the images taken with increased magnification (Fig. 2 B). It should be emphasized that regions of junction between neighboring cells were the regions of the plasmalemma, where PanX1 was first expressed after its expression in the ER membrane.

Intercellular  $\text{Ca}^{2+}$  wave propagation may generally involve a release of paracrine agents (such as ATP), which then activate receptors in neighboring cells triggering  $\text{Ca}^{2+}$  entry through  $\text{Ca}^{2+}$ -permeable membrane ion channels and/or  $\text{Ca}^{2+}$  release from the ER mediated by  $\text{IP}_3$  receptors ( $\text{IP}_3\text{Rs}$ ) and/or RyRs.  $\text{Ca}^{2+}$  entering the cell through gap junction channels can also activate RyRs, via a  $\text{Ca}^{2+}$ -induced  $\text{Ca}^{2+}$  release mechanism. To prevent the contribution of these mechanisms under our experimental conditions and to unmask changes in  $[\text{Ca}^{2+}]_i$  resulting solely from  $\text{Ca}^{2+}$  entry through gap junction channels, the cells were bathed in a  $\text{Ca}^{2+}$ -free solution supplemented with 300  $\mu\text{M}$  EGTA (to prevent  $\text{Ca}^{2+}$  entry from extracellular media), 0.5  $\mu\text{M}$  TG (to inhibit SERCA and deplete the ER), 100  $\mu\text{M}$  ryanodine (to inhibit RyRs), 100  $\mu\text{M}$  2-APB (to inhibit  $\text{IP}_3\text{Rs}$ ), and 5  $\mu\text{M}$  U-73122 (to inhibit phospholipase C and prevent  $\text{IP}_3$  formation). This experimental approach effectively blocked the paracrine pathway, which may otherwise have contributed to intercellular  $\text{Ca}^{2+}$  wave propagation. Indeed, no  $[\text{Ca}^{2+}]_i$  transients were observed in LNCaP cells in response to application of 50  $\mu\text{M}$  ATP after a 5-min incubation of the cells in this experimental media ( $n = 7$ ). Upon dialysis of the cell with  $\text{Ca}^{2+}$ -containing solutions, the  $\text{Ca}^{2+}$  movement rate from the dialyzed cell to the adjacent one was significantly greater in the LNCaP-PanX1 cells (Fig. 7 A;  $n = 8$ ; and Fig. 7 C;  $n = 34$ ) than in the LNCaP-EGFP cells (Fig. 7 D;  $n = 14$ ) or in the control LNCaP cells (Fig. 7 B;  $n = 12$ ; and Fig. 7 E;  $n = 13$ ). This is emphasized by the time course plots of the normalized fluo-4 (Fig. 7, A and B) or rhod-2 (Fig. 7, C and E) fluorescence and is summarized further in the histograms (Fig. 7 F), where a relative increase in rhod-2 fluorescence detected in the adjacent cell 8 min after the beginning of dialysis is presented as a percentage of that observed at this moment in the dialyzed cell. The relative increase in rhod-2 fluorescence in the adjacent cell caused solely by  $\text{Ca}^{2+}$  movement from the dialyzed cell was significantly ( $P < 0.0001$ ) higher in LNCaP-PanX1 cells ( $56.4 \pm 3.1\%$ ;  $n = 34$ ) than in LNCaP-EGFP cells ( $5.5 \pm 1.8\%$ ;  $n = 14$ ) or in control LNCaP cells ( $5.4 \pm 1.5\%$ ;  $n = 13$ ). It should be emphasized that it is extremely unlikely that intercellular  $\text{Ca}^{2+}$  movement under the experimental protocol used was mediated by hemichannels (but not by gap junction channels formed by PanX1) because no measurable  $\text{Ca}^{2+}$  entry from the patch pipette into the cell was detected in cell-attached configuration.

Finally, we examined whether the effects of overexpression of PanX1 in LNCaP-PanX1 cell line observed in our experiments may, in fact, be caused by modification of native connexin expression. Although only Cx32 mRNA has been previously demonstrated to be expressed at a low level in LNCaP cell line (Tate et al., 2006), it has been reported that overexpression of Cx32 or Cx43 may lead to functional gap junctions in this androgeno-dependent cell line (Mehta et al., 1999; Govindarajan et al., 2002). Therefore, we checked the expression of both Cx32 and Cx43 in a LNCaP-PanX1 cell line, LNCaP cells transiently transfected with PanX1, a control LNCaP cell line, and LNCaP cells transiently transfected with either Cx32 or Cx43. In agreement with what has previously been reported (Tate et al., 2006), we found no evidence for the expression of native Cx43 in any LNCaP cell types used in our experiments (unpublished data). Using Western blot analysis we did, however, detect a low but stable level of endogenous Cx32 protein in LNCaP cells (Fig. 8), which is in agreement with previously reported observations of Cx32 mRNA in this cell type (Tate et al., 2006). As expected, a higher level of Cx32 protein was detected in LNCaP cell after overexpression of Cx32 (Fig. 8). It should be emphasized, however, that the PanX-EGFP expression level was about 100 times higher than that of endogenous Cx32. Furthermore, immunodetection failed to reveal any native Cx32-forming gap junctions in either the LNCaP-PanX1 cell line or in control LNCaP cells (unpublished data).

In conclusion, our results strongly suggest that in our experimental model,  $\text{Ca}^{2+}$ -permeable gap junction channels were formed by PanX1, but not by connexin proteins.

## Discussion

Our study demonstrates for the first time that human PanX1, a protein encoded by a member of a new family of genes with yet unknown physiological role or roles, is a  $\text{Ca}^{2+}$ -permeable ion channel that is localized on both the ER and plasma membrane and participates in two physiologically important processes: the ER  $\text{Ca}^{2+}$  leak and intercellular  $\text{Ca}^{2+}$  movement.

Intercellular gap junction channels provide the primary pathway for communication between cells, which is crucial for coordination of tissue metabolism and sensitivity to extracellular stimuli. Where vertebrates are concerned, the integral membrane proteins forming intercellular channels are referred to as connexins. In insects and nematodes, this function has been attributed to proteins named innexins (Phelan et al., 1998). By homology with these invertebrate gap junction proteins, we predicted that another protein family, pannexins, might also form gap junctions (Panchin et al., 2000). Connexin channels have been demonstrated to cluster in maculae known as gap junctions and to allow cell-cell diffusion of ions (predominantly monovalent cations; for review see Nicholson et al., 2000) and small molecules. Presently, it is commonly agreed that connexins provide two major pathways for intercellular calcium signaling. The first one, an "intracellular" pathway, involves the passage of a  $\text{Ca}^{2+}$ -mobilizing messenger, such as  $\text{IP}_3$ , through gap-junctional connexins (Leybaert et al., 1998; Fry et al., 2001). The second one, an "extracellular" pathway, involves the

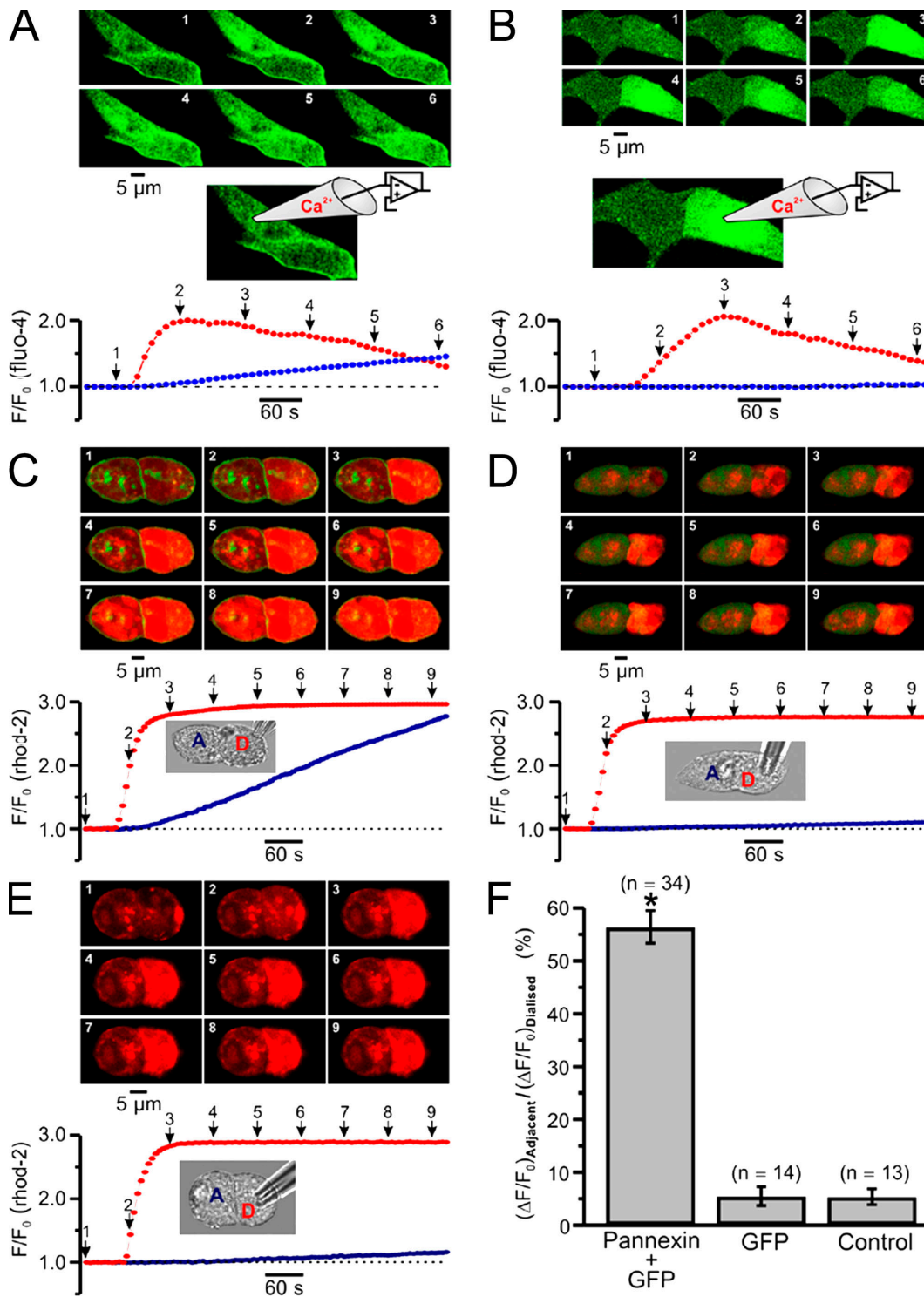


**Figure 7. PanX1 facilitates intercellular  $\text{Ca}^{2+}$  movement in LNCaP cells.** One of the two adjacent LNCaP cells from the line stably transfected with PanX1 coupled to EGFP (A and C), from the line stably transfected with EGFP only (D) and from the control line (B and E) was dialyzed through the patch pipette with solution containing either  $1 \mu\text{M}$   $\text{Ca}^{2+}$  (A and B) or  $100 \mu\text{M}$   $\text{Ca}^{2+}$  (C–F), while changes in the fluorescence of the  $\text{Ca}^{2+}$ -sensitive indicator fluo-4 (A and B) or rhod-2 (C–F), preloaded into the cells as AM ethers (see Materials and methods), were monitored in the dialyzed and adjacent cells using x–y confocal imaging. The cell membrane potential was clamped at  $-50$  mV. The pipette solution was composed of  $145$  mM KCl,  $10$  mM HEPES, and  $5$  mM glucose and was supplemented either with  $125 \mu\text{M}$   $\text{MgCl}_2$ ,  $3.8$  mM HEDTA, and  $0.3$  mM  $\text{CaCl}_2$  (to give a free  $\text{Ca}^{2+}$  concentration of  $1 \mu\text{M}$ ) or with  $2$  mM  $\text{MgCl}_2$  and  $100 \mu\text{M}$   $\text{CaCl}_2$ ; pH was adjusted to  $7.4$  with KOH. The cells were bathed in a solution composed of  $140$  mM NaCl,  $5$  mM KCl,  $2$  mM  $\text{MgCl}_2$ ,  $0.3$  mM  $\text{Na}_2\text{HPO}_4$ ,  $0.4$  mM  $\text{KH}_2\text{PO}_4$ ,  $4$  mM  $\text{NaHCO}_3$ ,  $5$  mM glucose, and  $10$  mM HEPES; pH adjusted to  $7.4$  with NaOH. Breakthrough (whole-cell configuration) was commenced during the x–y time series imaging protocol comprising  $100$ – $200$  frames each and acquired  $6$ – $10$  s apart. Note the fluorescence signal from GFP coupled to PanX1 that appears as a bright outline of the cell membranes in transfected LNCaP cells (image galleries in A and C). The plots below the image galleries illustrate the time course of the normalized fluorescence averaged within a total confocal optical slice of the dialyzed (red dotted line) and adjacent (blue dotted line) cells. The numbered arrows on the plots show the moments when the images presented above were captured. Please note a decline in the fluo-4 fluorescence in a dialyzed cell (A and B) reflecting a washout of fluo-4 into the patch pipette (containing a dye-free solution).

release of a purinergic messenger, such as ATP, through connexin hemichannels, and a subsequent activation of P2Y receptors in a paracrine way (Frame and de Feijter, 1997; Guthrie et al., 1999; Klepeis et al., 2001; Braet et al., 2003).

Although  $\text{Ca}^{2+}$  ions are recognized as second messengers within individual cells, their role as diffusible messengers in intercellular signaling has largely been overlooked because elevated  $[\text{Ca}^{2+}]_i$  has been shown to reduce gap-junctional conductance in several systems, including insects and vertebrates (Rose and Loewenstein, 1975; Spray and Bennett, 1985; Verselis et al., 2000). Indeed, it is now generally agreed that even if a small amount of  $\text{Ca}^{2+}$  can diffuse across gap junctions, it probably does not play a significant role in intercellular calcium signaling through connexin channels, which is mediated mainly by  $\text{IP}_3$  or other small signaling molecules (Churchill and Louis 1998; Niessen et al., 2000; Clair et al., 2001). This view is also supported by the recent observation that, in articular chondrocytes, intercellular calcium waves evoked by mechanical stimulation were abolished by incubation with TG and the phospholipase C inhibitor U73122 (D'Andrea et al., 2000). In contrast, in PanX1-transfected LNCaP cells an abrupt increase in  $[\text{Ca}^{2+}]_i$  evoked by dialysis of one cell through the patch pipette with solution containing high  $\text{Ca}^{2+}$  concentration (such an elevation of  $[\text{Ca}^{2+}]_i$  is expected to uncouple gap junction channels formed by connexins) caused an elevation of  $[\text{Ca}^{2+}]_i$  in adjacent cells, which was consistent with cell–cell  $\text{Ca}^{2+}$  diffusion via gap junction channels formed by pannexin. Indeed, intercellular  $\text{Ca}^{2+}$  movement was observed under conditions where the contribution of both the intracellular (or  $\text{IP}_3$ -dependent) and the extracellular pathway was eliminated by the inhibition of PLC and  $\text{IP}_3\text{Rs}$ , depletion of ER, and removal of  $\text{Ca}^{2+}$  from extracellular medium. Furthermore, the inability of LNCaP cells to respond to external ATP application (unpublished data) also argues against any possible involvement of an ATP-dependent extracellular pathway. Thus, our results suggest that pannexin proteins may form  $\text{Ca}^{2+}$ -permeable channels providing a pathway for intercellular  $\text{Ca}^{2+}$  diffusion.

Even more intriguing is our finding that pannexins may also function as “leak channels” in the ER membrane. Indeed, the ER is the major calcium store (Berridge and Irvine, 1989; Pozzan et al., 1994), and the  $\text{Ca}^{2+}$ -filling status of the ER controls many physiological processes, ranging from gene expression to apoptosis and proliferation (Bao et al., 2004). Under resting conditions, steady-state  $[\text{Ca}^{2+}]_L$  is determined by the dynamic equilibrium of two components; an active  $\text{Ca}^{2+}$  uptake mediated by ATP-dependent  $\text{Ca}^{2+}$  pumps of the SERCA family and passive  $\text{Ca}^{2+}$  efflux via leak channels. Even though this pump–leak cycle appears to be a common property of  $\text{Ca}^{2+}$ -storing organelles, little is known about the molecular nature of

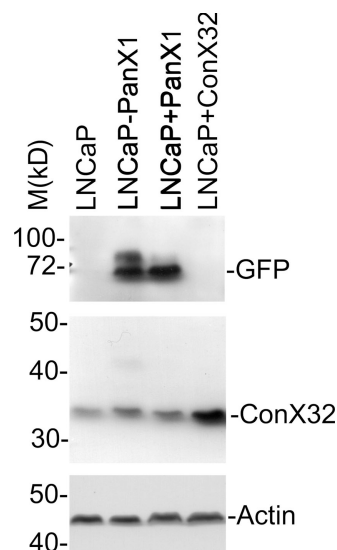


**Figure 8. PanX1 overexpression does not induce modification in Cx32 expression in LNCaP-PanX1 cell line.** Western-blot showing stable expression of Cx32 in control LNCaP cells (LNCaP), LNCaP cell line stably overexpressing PanX1-EGFP (LNCaP-PanX1), LNCaP cells transiently transfected with PanX1-EGFP for 3 d (LNCaP+PanX1), and Cx32-overexpressing LNCaP cells (LNCaP+Conx32). PanX1-EGFP detection was achieved with anti-EGFP antibody (top), Cx32 was detected with specific anti-Cx32 antibody and displayed a band of almost 32 kD (mid-dle), and finally actin was used for standardization of protein quantity. Note that native Cx32 is detected at the same level in LNCaP, LNCaP-PanX1, LNCaP+PanX1, and is, as expected, strongly expressed in LNCaP+Cx32. The experiment was reproduced twice.

the  $\text{Ca}^{2+}$ -leak pathway. Several mechanisms involving quite different proteins have been previously suggested to explain the basal  $\text{Ca}^{2+}$  leak from ER (for review see Camello et al., 2002), namely: (a) reverse  $\text{Ca}^{2+}$  flux through the pumps (Toyoshima and Nomura, 2002), (b)  $\text{Ca}^{2+}$  leak in neutral complexes with small molecules by translocon channels (Lomax et al., 2002; Van Coppenolle et al., 2004), (c) the fluxes of  $\text{Ca}^{2+}$  through “natural” ionophores, such as bile acids (Combettes et al., 1988; Zimniak et al., 1991), (d) an antiapoptotic protein Bcl-2–mediated  $\text{Ca}^{2+}$  leak (Pinton et al., 2000; Vanden Abeele et al., 2002; Bassik et al., 2004), and (e)  $\text{IP}_3\text{R}$ - or  $\text{RyR}$ -mediated  $\text{Ca}^{2+}$  leak (Oakes et al., 2005). However, as concluded by Camello et al. (2002), “the drawing of these mechanisms is only a fantasy map of the leak terra incognita and discovery of the exact mechanisms of calcium leak remains a challenge to scientists working in the calcium signaling field.” The results of our study strongly suggest that the heterologous expression of PanX1 in LNCaP and HEK cells dramatically reduces the ER  $\text{Ca}^{2+}$  content and alters the  $\text{Ca}^{2+}$  permeability of the ER membrane, which is consistent with an ion leak-channel function of PanX1 in the ER

This is not evident in the case of rhod-2 (C–E) which, being positively charged, is kept within the cell by several negatively charged molecules (and organelles). To unmask  $[\text{Ca}^{2+}]_i$  changes in adjacent cell caused solely by  $\text{Ca}^{2+}$  diffusion from the dialyzed cell, the cells were bathed in  $\text{Ca}^{2+}$ -free solution supplemented with 300  $\mu\text{M}$  EGTA (to prevent  $\text{Ca}^{2+}$  entry from extracellular media), 0.5  $\mu\text{M}$  TG (to inhibit SERCA and deplete the ER), 100  $\mu\text{M}$  ryanodine (to inhibit RyRs), 100  $\mu\text{M}$  2-APB (to inhibit  $\text{IP}_3\text{Rs}$ ), and 5  $\mu\text{M}$  U-73122 (to inhibit phospholipase C and prevent  $\text{IP}_3$  formation). The results are summarized in the histograms (F), where a relative increase in rhod-2 fluorescence detected in the adjacent cell 8 min after the beginning of dialysis is presented as a percentage of that observed at this moment in the dialyzed cell. Note that the relative increase in rhod-2 fluorescence in the adjacent was significantly ( $P < 0.0001$ ) higher in PanX1-EGFP-transfected cells than in cells transfected with EGFP only or in control cells.

membrane. To estimate the potential role of pannexins in endogenous ER basal  $\text{Ca}^{2+}$  leak, we used the siRNA and antisense hybrid depletion strategy for the endogenous PanX1 protein. Interestingly, in PanX1-depleted cells, the ER  $\text{Ca}^{2+}$  content was found to be  $\sim 40\%$  higher than in control cells. Moreover, the rate of the ER  $\text{Ca}^{2+}$  leak (unmasked by inhibition of SERCA-mediated  $\text{Ca}^{2+}$  uptake with TG) was substantially reduced in PanX1-depleted cells, thus, suggesting an important contribution of endogenous PanX1 to the global ER basal  $\text{Ca}^{2+}$  leak. One may speculate that reduced resting concentration of calcium in the ER associated with the PanX1 overexpression could be caused by the following: (a) the modified level of the BCL-2 family of proteins with ER localization and known to play an important role in the regulation of the calcium leak from the ER, (b) the increased level of the antiapoptotic protein BCL-2 (Pinton et al., 2000; Vanden Abeele et al., 2002; Bassik et al., 2004), and/or (c) the deficiency for two “multidomain” proapoptotic proteins Bax and Bak (Scorrano et al., 2003; Oakes et al., 2005). Our results show that the levels of these proteins expression were not changed by PanX1 overexpression, thereby suggesting that the PanX1 may mediate  $\text{Ca}^{2+}$  leak by itself, independently of other potential ER leak modulators. In this respect, it would be interesting to investigate whether the function of a pannexin, such as the ER  $\text{Ca}^{2+}$ -leak channel, is specific to vertebrates, or if, in fact, some invertebrate innexins (which are pannexin homologous) share this function.

In conclusion, this study directly demonstrates the involvement of PanX1 in intra- and intercellular  $\text{Ca}^{2+}$  signaling, thus, illustrating the multifunctional role of a single molecule.

## Materials and methods

### Plasmid construction

PanX1 cDNA encompassing the entire coding region was synthesized by PCR amplification of the cDNA clone (Panchin et al., 2000) using two gene-specific primers. A sense primer, containing a HindIII site at its 5'-end (PanX1F: 5'-TGTAAGCTTGCCATGGCCATCGCTCAAC-3'), and an antisense primer, containing an EcoRI site at its 5'-end (PanX1R: 5'-TGTAAT-TCACAGAAGTCTCTGTCGGGC-3'), were used. 500 ng of the pEGFP-N1 vector (CLONTECH Laboratories, Inc.) and PCR product were digested by HindIII and EcoRI. The digested vector and the PCR products were gel purified, ligated together, and cloned. The cDNA insert was sequenced to verify its identity and absence of mutation. Cx43-EGFP was a gift from B. Rose (Marine Biology laboratory, Woods Hole, MA), and Cx32 was a gift from M. Mesnil (University de Poitiers, Poitiers, France).

### Cell lines

The procedures for culturing and preparing LNCaP cells (American Type Culture Collection) for fluorescence measurements are detailed elsewhere (Vanden Abeele et al., 2002). HEK-293 cells were grown in DME, containing 10% FCS, 2 mM L-glutamine, and 100  $\mu\text{g}/\text{ml}$  kanamycin at 37°C in a humidity-controlled incubator with 5%  $\text{CO}_2$ .

### Transient expression in HEK-293 cells

HEK-293 cells (50% confluent) were transiently transfected by 2  $\mu\text{g}$  of plasmid (pEGFP-N1 or pannexin-pEGFP-N1), using a transfection reagent (Gene Porter 2; Gene Therapy Systems, Inc.) for 8 h in a serum-free medium. DME with 10% FBS was added overnight. Chimera expression was assessed by GFP fluorescence.

### Construction of a stable LNCaP cell line expressing PanX1-GFP: LNCaP-PanX cells

Stable cell lines expressing PanX1-EGFP protein were constructed by transfection with 2  $\mu\text{g}$  of pEGFP-N1/PanX1 plasmid in a 6-well plate for 6 h using a Gene Porter 2 reagent, following the manufacturer's recommended

protocol. The cells in culture were then maintained under selected pressures with 700  $\mu\text{g}/\text{ml}$  G418 for 4 wk. Colonies expressing GFP were identified under fluorescence microscope, subcloned, and maintained under the selected pressure for at least 3 wk.

### siRNA and ODN assays

LNCaP, LNCaP-PanX, or HEK cells were transfected overnight by either 5 or 100 nM siRNA anti-PanX1 mRNA (siRNA PanX), using Gene Porter 2 transfection reagent in 35-mm dishes for electrophysiological purpose or in 60-mm dishes for either RNA or protein extraction. Ready-to-use siRNA-AR (processing option: A4) was synthesized by Dharmaco, Inc. Location of either siRNA or ODNs refer to PanX1 cDNA from NM\_015368.3. The sense sequence of siRNA-PanX1 and siRNA mTRPC6 used were 5'-ACGA-UUUGAGCCUCUACAA(dTdT)-3' (1362–1380) and 5'-UAAUUGCCGAG-ACCG UUCAU(dTdT)-3' (1591–1609, accession no.: NM\_013838.1), respectively. Phosphorothioate ODNs were produced by Eurogentec and used at 0.5  $\mu\text{M}$ . Antisense sequences used were 5'-TATGCAGCCAC-AGTGGGAGG-3' (685–704) and 5'-TCAGATACCTCCACAAACT-3' (929–948), although the sense sequence used was 5'-CCTCCCACTGTG-GCTGCATA-3'.

### Analysis of PanX1 expression (RT-PCR)

Total RNA was isolated from different cell lines using the guanidium thiocyanate-phenol-chloroform extraction procedure (Chomczynski and Sacchi, 1987). After a DNase I (Life Technologies) treatment to eliminate genomic DNA, 2  $\mu\text{g}$  of total RNA was reverse transcribed into cDNA at 42°C using random hexamer primers (Perkin Elmer) and MuLV reverse transcriptase (Perkin Elmer) in a 20- $\mu\text{l}$  final volume, followed by PCR. The PCR primers used to amplify pannexin cDNAs were designed with Gene Runner 3.05 (Hastings Software). Primers for the human pannexin synthesized by Life Technologies were as follows: forward 5'-CCCAATTGTGGAGCAGTACT-TG-3' (963–984) and reverse 5'-AGACACTTGTATGAC TTGACCTCAC-3' (1403–1427). The expected DNA length of the PCR product generated by these primers was 465 bp (NM\_015368, National Center for Biotechnology Information database). PCR was performed on the RT-generated cDNA using a thermal cycler (GeneAmp PCR System 2400; Perkin Elmer). To detect pannexin cDNAs, PCR was performed by adding 1  $\mu\text{l}$  of the RT template to a mixture of (final concentrations): 50 mM KCl, 10 mM Tris-HCl, pH 8.3, 2.5 mM  $\text{MgCl}_2$ , 200  $\mu\text{M}$  of each dNTP, 600 nM of sense and antisense primers, and 1 U AmpliTaq Gold (Perkin Elmer) in a final volume of 25  $\mu\text{l}$ . DNA amplification conditions included an initial 5-min denaturation step at 95°C (which also activated the Gold variant of Taq Polymerase) and 35 cycles of 30 s at 95°C, 30 s at 60°C, 40 s at 72°C, and finally, 5 min at 72°C.

### Western blot assay

LNCaP-PanX cells (vehicle or siRNA-transfected) were harvested and pelleted in PBS and then sonicated in ice-cold buffer, pH 7.2, containing the following: 10 mM  $\text{PO}_4\text{Na}_2/\text{K}$  buffer, 150 mM NaCl, 1 g/100 ml sodium deoxycholate, 1% Triton X-100, 1% NP-40, a mixture of protease inhibitors (Sigma-Aldrich), and a phosphatase inhibitor (sodium orthovanadate; Sigma-Aldrich). Samples were electrophoretically analyzed on a 10% polyacrylamide gel using the SDS-PAGE technique. The proteins were then transferred for 1 h (50 mA, 25 V) onto a nitrocellulose membrane using a semidry electrobloater (Bio-Rad Laboratories). The membrane was then cut into thin, equally sized strips and processed for Western blot. The strips were blocked in 5% TNT-milk (15 mM Tris buffer, pH 8.0, 140 mM NaCl, 0.05% Tween 20, and 5% non-fat dry milk) for 30 min at room temperature, washed three times in TNT, soaked in primary antibody anti-GFP (CHEMICON International, Inc.), anti-actin (MS-1295-P; Neomarkers), anti-Cx32 (CHEMICON International, Inc.), or anti-Cx43 (CHEMICON International, Inc.), and then diluted 1:500, 1:500, 1:200, and 1:200, respectively, in TNT-milk for 1 h at room temperature. After three washes in TNT, the strips were transferred into the IgG horseradish peroxidase-linked secondary antibodies (CHEMICON International, Inc.), and diluted in TNT-milk (1:20,000) for 1 h. After three 10-min washes in TNT, the strips were processed for chemiluminescent detection using chemiluminescent substrate (Supersignal West Pico; Pierce Chemical Co.) according to the manufacturer's instructions. The blots were then exposed to X-Omat AR films (Eastman Kodak Company).

### Preparation of PanX1-EGFP transfected cells for confocal analysis

LNCaP cells were transfected at 60% confluency, as described in Transient expression in HEK-293 cells, in 6-well plates. After two washes in PBS,

cells were fixed with 4% formaldehyde-1X PBS for 15 min. After two washes in PBS, the slides were mounted with Mowiol.

#### Fluorescence measurements of $[Ca^{2+}]_i$ and $[Ca^{2+}]_t$

Fluorescence imaging was performed in HBSS solution containing 142 mM NaCl, 5.6 mM KCl, 1 mM  $MgCl_2$ , 0–10 mM  $CaCl_2$ , 0.34 mM  $Na_2HPO_4$ , 0.44 mM  $KH_2PO_4$ , 10 mM Hepes, and 5.6 mM glucose. The osmolarity and pH of external solutions were adjusted to 310 mosM  $l^{-1}$  and 7.4, respectively.

Cytosolic calcium concentration was measured using fura-2-loaded cells. LNCaP cells were loaded for 45 min at room temperature with 2  $\mu$ M fura-2-AM prepared in HBSS and, subsequently, washed three times with the same dye-free solution. The coverslip was then transferred into a perfusion chamber on a microscope (IX70; Olympus) equipped for fluorescence. Fluorescence was alternatively excited at 340 and 380 nm with a monochromator (Polychrome IV; TILL Photonics) and was captured after filtration through a long-pass filter (510 nm) by a 5 MHz charge-coupled device camera (MicroMax; Princeton Instruments). Acquisition and analysis were performed with the Metafluor 4.5 software (Universal Imaging Corp.). The intracellular calcium concentration was derived from the ratio of the fluorescence intensities for each of the excitation wavelengths (F340/F380) and from the equation of Grynkiewicz et al. (1985). All recordings were performed at room temperature. The cells were continuously perfused with the HBSS solution, and chemicals were added via the perfusion system. The flow rate of the whole-chamber perfusion system was set to 1 ml/min, and the chamber volume was 500  $\mu$ l.

$[Ca^{2+}]_t$  was monitored using Mag-fura-2 as previously described (Vanden Abeele et al., 2002).

#### Confocal microscopy

The HEK-293 and LNCaP cells were grown on coverslips and transfected with pannexin-pEGFP-N1. Fluorescence imaging was performed using a confocal scanner (488 nm excitation for GFP; LSM 510; Carl Zeiss Micro-Imaging, Inc.) based on an Axiovert 200 M motorized inverted microscope with a plan-Apochromat 63 $\times$ , 1.4 NA, oil immersion objective (Carl Zeiss MicroImaging, Inc.). The confocal microscope software used was AIM 3.2 (Carl Zeiss MicroImaging, Inc.). Confocal  $[Ca^{2+}]_i$  imaging in LNCaP cells was performed using  $Ca^{2+}$ -sensitive indicators fluo-4 or rhod-2. Fluo-4 was loaded by 20-min exposure of the cells to 5  $\mu$ M fluo-4 AM (diluted from a stock containing 2 mM fluo-4 AM and 0.025 [wt/vol] pluronic F-127 in dimethyl sulphoxide) at room temperature, followed by a 40-min wash to allow time for deesterification. Rhod-2 was loaded by 10-min incubation of the cells with 15  $\mu$ M rhod-2 AM (diluted from a stock containing 1 mM rhod-2 AM and 0.025 [wt/vol] pluronic F-127 in dimethyl sulphoxide) at room temperature, followed by a 60-min wash. Rhod-2 fluorescence was excited by the 543-nm line of a 5-mW HeNe ion laser and the emitted fluorescence was captured at wavelengths above 560 nm. Fluo-4 and GFP fluorescence were excited by the 488-nm line of a 20 mW argon ion laser and the fluorescence emitted was detected at wavelengths >505 nm. For both desired laser lines, the illumination intensity was set with an acoustooptical tunable filter. In the experiments on the imaging of intercellular  $Ca^{2+}$  movement, one of the two adjacent LNCaP cells was dialyzed through the patch pipette with solution containing either 1  $\mu$ M  $Ca^{2+}$  (pipette solution: 145 mM KCl, 10 mM Hepes, 5 mM glucose, 125  $\mu$ M  $MgCl_2$ , 3.8 mM HEDTA, and 0.3 mM  $CaCl_2$ ; pH 7.4 with KOH) or 100  $\mu$ M  $Ca^{2+}$  (pipette solution: 145 mM KCl, 10 mM Hepes, 5 mM glucose, 2 mM  $MgCl_2$ , and 100  $\mu$ M  $CaCl_2$ ; pH 7.4 with KOH), while changes in the fluorescence of the  $Ca^{2+}$ -sensitive indicator were monitored in the dialyzed and adjacent cells using x-y confocal imaging. To unmask  $Ca^{2+}$  diffusion from the dialyzed to the adjacent cell,  $Ca^{2+}$  entry from extracellular media was prevented by incubation of the cells in  $Ca^{2+}$ -free solution supplemented with 300  $\mu$ M EGTA, (bath solution: 140 mM NaCl, 5 mM KCl, 2 mM  $MgCl_2$ , 0.3 mM  $Na_2HPO_4$ , 0.4  $KH_2PO_4$ , 4 mM  $NaHCO_3$ , 5 mM glucose, and 10 mM Hepes; pH adjusted to 7.4 with NaOH), whereas  $Ca^{2+}$  release from the ER was prevented by the following: (a) ER depletion with 0.5  $\mu$ M TG, (b) blocking RyRs with 100  $\mu$ M ryanodine, (c) IP $_3$ Rs blocking with 100  $\mu$ M 2-APB, and (d) PLC inhibition with 5  $\mu$ M U-73122.

Spatial organization of the ER was visualized using selective ER marker BODIPY 558/568 brefeldin A (Deng et al., 1995; White and McGeown, 2002; Oh-hashi et al., 2003). The ER was stained by 10–30 min incubation of the cells at room temperature in the solution containing 0.1–0.5 mM of the dye. The fluorescence was excited by the 543-nm line of a 5-mW HeNe ion laser, and the emitted fluorescence was captured at wavelengths >560 nm. To visualize the fine spatial pattern of the BODIPY 558/568 brefeldin A and EGFP fluorescence, the fluorescent signal was collected from the confocal optical slice below 0.5  $\mu$ m with x-y frame size of 2048  $\times$  2048 pixels, and the final images were obtained as a result of

averaging of four sequential images taken in multitrack (line-by-line acquisition) configuration of the confocal scanner followed by low-pass filtering ( $7 \times 7$  pixels; LSM 510 software) to improve the signal-to-noise ratio.

#### Chemicals

All chemicals were obtained from Sigma-Aldrich, except for fura-2-AM and TG, which were purchased from Calbiochem, and Mag-fura-2-AM, Fluo-4-AM, Rhod-2, and BODIPY 558/568 brefeldin A, which were obtained from Invitrogen.

#### Data analysis and statistics

Each experiment was repeated several times. The data were analyzed using Origin 5.0 (Microcal) software. Results were expressed as the mean  $\pm$  the SEM where appropriate. The *t* test was used for statistical comparison of the differences, and *P* < 0.05 was considered significant.

We are grateful to Dr. B. Rose for the gift of Cx43-EGFP. We are grateful to Dr. M. Mesnil for the gift of Cx32.

This work was supported by grants from Institut National de la Santé et de la Recherche Médicale, the Ministère de l'Éducation Nationale, the Ligue Nationale Contre le Cancer, the International Association for Cooperation with Scientists from the former Soviet Union, the Fondation pour la Recherche Médicale, the Wellcome Trust (grants 060659 and 075112), and the Russian Foundation for Basic Research (grants 05-04-48401 and 06-04-63043).

Submitted: 23 January 2006

Accepted: 13 July 2006

## References

- Bao, L., S. Locovei, and G. Dahl. 2004. Pannexin membrane channels are mechanosensitive conduits for ATP. *FEBS Lett.* 572:65–86.
- Baranova, A., D. Ivanov, N. Petrash, A. Pestova, M. Skoblov, I. Kelmanson, D. Shagin, S. Nazarenko, E. Geraymovych, O. Litvin, et al. 2004. The mammalian pannexin family is homologous to the invertebrate innexin gap-junction proteins. *Genomics.* 83:706–716.
- Bassik, M.C., L. Scorrano, S.A. Oakes, T. Pozzan, and S.J. Korsmeyer. 2004. Phosphorylation of BCL-2 regulates ER  $Ca^{2+}$  homeostasis and apoptosis. *EMBO J.* 23:1207–1216.
- Berridge, M.J., and R.F. Irvine. 1989. Inositol phosphates and cell signaling. *Nature.* 341:197–205.
- Braet, K., W. Vandamme, P.E. Martin, W.H. Evans, and L. Leybaert. 2003. Photoliberating inositol-1,4,5-trisphosphate triggers ATP release that is blocked by the connexin mimetic peptide gap 26. *Cell Calcium.* 33:37–48.
- Bruzzone, R., S.G. Hormuzdi, M.T. Barbe, A. Herb, and H. Monyer. 2003. Pannexins, a family of gap junction proteins expressed in brain. *Proc. Natl. Acad. Sci. USA.* 100:13644–13649.
- Camello, C., R. Lomax, O.H. Petersen, and A.V. Tepikin. 2002. Calcium leak from intracellular stores—the enigma of calcium signaling. *Cell Calcium.* 32:355–361.
- Chomczynski, P., and N. Sacchi. 1987. Single-step method of RNA isolation by acid guanidinium thiocyanate-phenol-chloroform extraction. *Anal. Biochem.* 162:156–159.
- Churchill, G.C., and C.F. Louis. 1998. Roles of  $Ca^{2+}$ , inositol trisphosphate and cyclic ADP-ribose in mediating intercellular  $Ca^{2+}$  signaling in sheep lens cells. *J. Cell Sci.* 111:1217–1225.
- Clair, C., C. Chalumeau, T. Tordjmann, J. Poggioli, C. Erneux, G. Dupont, and L. Combettes. 2001. Investigation of the roles of  $Ca^{2+}$  and InsP(3) diffusion in the coordination of  $Ca^{2+}$  signals between connected hepatocytes. *J. Cell Sci.* 114:1999–2007.
- Combettes, L., M. Dumont, B. Berthon, S. Erlinger, and M. Claret. 1988. Release of calcium from the endoplasmic reticulum by bile acids in rat liver cells. *J. Biol. Chem.* 263:2299–2303.
- D'Andrea, P., A. Calabrese, I. Capozzi, M. Grandolfo, R. Tonon, and F. Vittur. 2000. Intercellular  $Ca^{2+}$  waves in mechanically stimulated articular chondrocytes. *Biorheology.* 37:75–83.
- Deng, Y., J.R. Bannink, H.C. Kang, R.P. Haugland, and J.W. Yewdell. 1995. Fluorescent conjugates of brefeldin A selectively stain the endoplasmic reticulum and Golgi complex of living cells. *J. Histochem. Cytochem.* 43:907–915.
- Foyouzi-Youssefi, R., S. Arnaudeau, C. Borner, W.L. Kelley, J. Tschopp, D.P. Lew, N. Demaurex, and K.H. Krause. 2000. Bcl-2 decreases the free  $Ca^{2+}$  concentration within the endoplasmic reticulum. *Proc. Natl. Acad. Sci. USA.* 97:5723–5728.

- Frame, M.K., and A.W. de Feijter. 1997. Propagation of mechanically induced intercellular calcium waves via gap junctions and ATP receptors in rat liver epithelial cells. *Exp. Cell Res.* 230:197–207.
- Fry, T., J.H. Evans, and M.J. Sanderson. 2001. Propagation of intercellular calcium waves in C6 glioma cells transfected with connexins 43 or 32. *Microsc. Res. Tech.* 52:289–300.
- Govindarajan, R., S. Zhao, X.H. Song, R.J. Guo, M. Wheelock, K.R. Johnson, and P.P. Mehta. 2002. Impaired trafficking of connexins in androgen-independent human prostate cancer cell lines and its mitigation by alpha-catenin. *J. Biol. Chem.* 277:50087–50097.
- Grynkiewicz, G., M. Poenie, and R.Y. Tsien. 1985. A new generation of  $\text{Ca}^{2+}$  indicators with greatly improved fluorescence properties. *J. Biol. Chem.* 260:3440–3450.
- Guthrie, P.B., J. Knappenberger, M. Segal, M.V. Bennett, A.C. Charles, and S.B. Kater. 1999. ATP released from astrocytes mediates glial calcium waves. *J. Neurosci.* 19:520–528.
- Khvorova, A., A. Reynolds, and S.D. Jayasena. 2003. Functional siRNAs and miRNAs exhibit strand bias. *Cell.* 115:209–216.
- Klepeis, V.E., A. Cornell-Bell, and V. Trinkaus-Randall. 2001. Growth factors but not gap junctions play a role in injury-induced  $\text{Ca}^{2+}$  waves in epithelial cells. *J. Cell Sci.* 114:4185–4195.
- Kumar, N.M., D.S. Friend, and N.B. Gilula. 1995. Synthesis and assembly of human beta 1 gap junctions in BHK cells by DNA transfection with the human beta 1 cDNA. *J. Cell Sci.* 108:3725–3734.
- Leybaert, L., K. Paemeleire, A. Strahonja, and M.J. Sanderson. 1998. Inositol trisphosphate-dependent intercellular calcium signaling in and between astrocytes and endothelial cells. *Glia.* 24:398–407.
- Lomax, R.B., C. Camello, F. Van Coppenolle, O.H. Petersen, and A.V. Tepikin. 2002. Basal and physiological  $\text{Ca}^{2+}$  leak from the endoplasmic reticulum of pancreatic acinar cells. Second messenger-activated channels and translocons. *J. Biol. Chem.* 277:26479–26485.
- Mehta, P.P., C. Perez-Stable, M. Nadji, M. Mian, K. Asotra, and B.A. Roos. 1999. Suppression of human prostate cancer cell growth by forced expression of connexin genes. *Dev. Genet.* 24:91–110.
- Nicholson, B.J., P.A. Weber, F. Cao, H. Chang, P. Lampe, and G. Goldberg. 2000. The molecular basis of selective permeability of connexins is complex and includes both size and charge. *Braz. J. Med. Biol. Res.* 33:369–378.
- Niessen, H., H. Harz, P. Bedner, K. Kramer, and K. Willecke. 2000. Selective permeability of different connexin channels to the second messenger inositol 1,4,5-trisphosphate. *J. Cell Sci.* 113:1365–1372.
- Oakes, S.A., L. Scorrano, J.T. Opferman, M.C. Bassik, M. Nishino, T. Pozzan, and S.J. Korsmeyer. 2005. Proapoptotic BAX and BAK regulate the type 1 inositol trisphosphate receptor and calcium leak from the endoplasmic reticulum. *Proc. Natl. Acad. Sci. USA.* 102:105–110.
- Oh-hashii, K., Y. Naruse, F. Amaya, G. Shimosato, and M. Tanaka. 2003. Cloning and characterization of a novel GRP78-binding protein in the rat brain. *J. Biol. Chem.* 278:10531–10537.
- Panchin, Y. 2005. Evolution of gap junction proteins—the pannexin alternative. *J. Exp. Biol.* 208:1415–1419.
- Panchin, Y., I. Kelmanson, M. Matz, K. Lukyanov, N. Usman, and S. Lukyanov. 2000. A ubiquitous family of putative gap junction molecules. *Curr. Biol.* 10:R473–R474.
- Phelan, P., J.P. Bacon, J.A. Davies, L.A. Stebbings, M.G. Todman, L. Avery, R.A. Baines, T.M. Barnes, C. Ford, S. Hekimi, et al. 1998. Innexins: a family of invertebrate gap-junction proteins. *Trends Genet.* 14:348–349.
- Pinton, P., D. Ferrari, P. Magalhaes, K. Schulze-Osthoff, F. Di Virgilio, T. Pozzan, and R. Rizzuto. 2000. Reduced loading of intracellular  $\text{Ca}^{2+}$  stores and downregulation of capacitative  $\text{Ca}^{2+}$  influx in Bcl-2-overexpressing cells. *J. Cell Biol.* 148:857–862.
- Pozzan, T., R. Rizzuto, P. Volpe, and J. Meldolesi. 1994. Molecular and cellular physiology of intracellular calcium stores. *Physiol. Rev.* 74:595–636.
- Rose, B., and W.R. Loewenstein. 1975. Permeability of cell junction depends on local cytoplasmic calcium activity. *Nature.* 254:250–252.
- Scorrano, L., S.A. Oakes, J.T. Opferman, E.H. Cheng, M.D. Sorcinelli, T. Pozzan, and S.J. Korsmeyer. 2003. BAX and BAK regulation of endoplasmic reticulum  $\text{Ca}^{2+}$ : a control point for apoptosis. *Science.* 300:135–139.
- Spray, D.C., and M.V. Bennett. 1985. Physiology and pharmacology of gap junctions. *Annu. Rev. Physiol.* 47:281–303.
- Stout, C., D.A. Goodenough, and D.L. Paul. 2004. Connexins: functions without junctions. *Curr. Opin. Cell Biol.* 16:507–512.
- Tate, A.W., T. Lung, A. Radhakrishnan, S.D. Lim, X. Lin, and M. Edlund. 2006. Changes in gap junctional connexin isoforms during prostate cancer progression. *Prostate.* 66:19–31.
- Toyoshima, C., and H. Nomura. 2002. Structural changes in the calcium pump accompanying the dissociation of calcium. *Nature.* 418:605–611.
- Vanden Abeele, F., R. Skryma, Y. Shuba, F. Van Coppenolle, C. Slomianny, M. Roudbaraki, B. Mauroy, F. Wuytack, and N. Prevarskaya. 2002. Bcl-2-dependent modulation of  $\text{Ca}^{2+}$  homeostasis and store-operated channels in prostate cancer cells. *Cancer Cell.* 1:169–179.
- Van Coppenolle, F., F. Vanden Abeele, C. Slomianny, M. Flourakis, J. Hesketh, E. Dewailly, and N. Prevarskaya. 2004. Ribosome-translocon complex mediates calcium leakage from endoplasmic reticulum stores. *J. Cell Sci.* 117:4135–4142.
- Verselis, V.K., E.B. Trexler, and F.F. Bukauskas. 2000. Connexin hemichannels and cell-cell channels: comparison of properties. *Braz. J. Med. Biol. Res.* 33:379–389.
- Willecke, K., J. Eiberger, J. Degen, D. Eckardt, A. Romualdi, M. Guldenagel, U. Deutsch, and G. Sohl. 2002. Structural and functional diversity of connexin genes in the mouse and human genome. *J. Biol. Chem.* 277:725–737.
- White, C., and G. McGeown. 2002. Imaging of changes in sarcoplasmic reticulum  $[\text{Ca}^{2+}]$  using Oregon Green BAPTA 5N and confocal laser scanning microscopy. *Cell Calcium.* 31:151–159.
- Zimniak, P., J.M. Little, A. Radomska, D.G. Oelberg, M.S. Anwer, and R. Lester. 1991. Taurine-conjugated bile acids act as  $\text{Ca}^{2+}$  ionophores. *Biochemistry.* 30:8598–8604.